Frequency shift and mode coupling of the collective modes of superfluid Fermi gases in the BCS-BEC crossover

Yu Zhou and Wen Wen
Department of Physics and Institute of Theoretical Physics, East China Normal University, Shanghai 200062, China

Guoxiang Huang*
State Key Laboratory of Precision Spectroscopy and Department of Physics, East China Normal University, Shanghai 200062, China
(Received 30 December 2007; published 25 March 2008)

We investigate the dynamical behavior of large-amplitude collective modes in a superfluid Fermi gas in the crossover from Bardeen–Cooper–Schrieffer (BCS) superfluid to Bose–Einstein condensate (BEC) based on a hydrodynamic approach. We first solve the superfluid hydrodynamic equations that describe the time evolution of fermionic condensates in the BCS-BEC crossover and calculate explicitly the frequency shifts of the collective modes induced by nonlinear effects using the Lindstedt–Poincaré method. The result shows that the frequency shifts display different features in different superfluid regimes. We then study the second-harmonic generation of the collective modes under a phase-matching condition, which can be fulfilled by choosing appropriate parameters of the system. The analytical results obtained are checked by numerical simulations and good agreement is found.

DOI: 10.1103/PhysRevB.77.104527 PACS number(s): 03.75.Kk

I. INTRODUCTION

In recent years, much attention has been paid to the study of the crossover from Bardeen–Cooper–Schrieffer (BCS) superfluid to Bose–Einstein condensation (BEC), a topic not only of fundamental interest in condensed matter theory but also closely related to the understanding of physical mechanism for high-T_c superconductivity.[1–4] Ultracold quantum degenerate gases of fermionic atoms (such as ^{6}Li and ^{40}K, and ^{173}Yb)[5] with tunable interparticle interaction offer an excellent opportunity for deep exploration on the property of BCS-BEC crossover in a controllable way. Experimentally, condensed fermionic atomic pairs in the regimes of BEC,[6] BCS,[7] and their crossover[8] have been observed and their various superfluid properties have been investigated in detail recently by using a magnetic-field-induced Feshbach resonance.[4]

At low temperature, collective modes are most important excitations that can be used to characterize dominant physical property of system. Since the successfully experimental realization of fermionic condensates, considerable interest has focused on the study of the collective modes in ultracold quantum degenerate Fermi gases. By means of the Feshbach resonance, the interparticle interaction, characterized by s-wave scattering length, can be tuned from large positive to large negative values, providing a possibility to investigate the nonlinear nature of collective modes in various superfluid regimes. However, to the best of our knowledge, up to now all works on the collective modes in superfluid Fermi gases in the BCS-BEC crossover have concentrated mainly on their linear behavior.[4,9–30] It is necessary to consider nonlinear effects of collective modes when large-amplitude oscillations in fermionic condensates are created. In this work, by directly generalizing the work of Dalfovo *et al.*[31] for bosonic condensates, we investigate the nonlinear dynamics of superfluid Fermi gases from BCS superfluid to Bose–Einstein condensation based on a simple superfluid hydrodynamic approach.[23–30] We are interested in especially specific features of frequency shifts and resonant mode couplings of the collective modes in a fermionic condensate due to the nonlinear effect of the system.

This paper is organized as follows. In Sec. II, we give a simple introduction to the superfluid hydrodynamic equations valid in the whole BCS-BEC crossover and present the solutions of linear collective modes of the system. In Sec. III, by using the Lindstedt–Poincaré method, we make an explicit calculation on the frequency shifts of the collective modes induced by nonlinear effects and discuss their physical properties in different superfluid regimes. In Sec. IV, we study the second-harmonic generation (SHG) of the collective modes under a phase-matching condition, which can be fulfilled by choosing suitable parameters of the system. We provide also numerical simulations on the second-harmonic generation in different superfluid regimes and good agreement with analytical result is found. Finally, we summarize our main results in Sec. V.

II. LINEAR COLLECTIVE EXCITATIONS

A. Superfluid hydrodynamic equations

Consider a superfluid Fermi gas in which fermionic atoms have two different internal states and the atomic numbers for both the internal states are equal. By means of the Feshbach resonance, a crossover from BCS to BEC regimes can be realized through tuning an applied magnetic field, and hence changing the s-wave scattering length a_s. When $a_s<0$ ($a_s>0$), the system is in a BCS (BEC) regime. By defining a dimensionless interaction parameter $\eta \equiv 1/(k_F a_s)$, where $k_F=(3\pi^2 n)^{1/3}$ is Fermi wave number with n being the atomic density, one can distinguish several different superfluid regimes,[23–30] i.e., BCS regime ($\eta<-1$), BEC regime ($\eta>1$), and BCS-BEC crossover regime ($-1<\eta<1$). $\eta=-\infty$ ($\eta=+\infty$) is called BCS (BEC) limit and $\eta=0$ is called

unitarity limit. Both theoretical and experimental studies show that the transition from the BCS regime to the BEC regime is smooth.[2,4] Thus, one can study the physical property of the system in various superfluid regimes in a simple and unified way.

There are several theoretical approaches for the study of collective modes in superfluid Fermi gases in the BCS-BEC crossover. One of them is microscopic theory, in which single-channel (Fermi-only) or two-channel (Fermi–Boson) model Hamiltonians with Fermi or Fermi–Boson degrees of freedom are used (see Refs. 2 and 4 and references therein). However, because in most experiments superfluid Fermi gas is confined by a trapping potential, the inhomogeneous character of the system makes the microscopic approaches difficult. Notice that at very low temperature (around 10^{-8} K), low-energy collective modes cannot decay by formation of single fermionic excitations because of the gap in their energy spectrum. Thus, thermal excitations play no significant role and the system can be taken as a perfect superfluid. In this situation, the dynamics of the collective excitations in the system can be well described by macroscopic superfluid hydrodynamics,[23–30] whose theoretical treatment is relatively simple and direct in comparison with the microscopic approaches.

The macroscopic dynamics of the superfluid at zero temperature is governed by the hydrodynamic equations[4]

$$\frac{\partial n}{\partial t} + \nabla \cdot (n\mathbf{v}) = 0, \tag{1a}$$

$$m\frac{\partial \mathbf{v}}{\partial t} + \nabla\left[\frac{1}{2}m\mathbf{v}^2 + \mu(n) + V_{\text{ext}}(\mathbf{r})\right] = 0, \tag{1b}$$

where $\mathbf{v}$ is superfluid velocity, m is atomic mass, and $V_{\text{ext}}(\mathbf{r})$ is a harmonic trapping potential. The equation of state (also called bulk chemical potential) under a local density approximation has the form $\mu(n)=\partial[n\varepsilon(n)]/\partial n$, where $\varepsilon(n)$ is the bulk energy per particle. Introducing $\varepsilon(n)=(3/5)\varepsilon_F\sigma(\eta)$, with $\varepsilon_F=\hbar^2k_F^2/(2m)$ being Fermi energy, one obtains[24–30]

$$\mu(n) = \varepsilon_F\left[\sigma(\eta) - \frac{\eta}{5}\frac{\partial\sigma(\eta)}{\partial\eta}\right]. \tag{2}$$

The function $\sigma(\eta)$ can be obtained by fitting the data by Monte Carlo calculations.[32,33] An explicit expression for ^{6}Li has been provided in Ref. 24. Usually, as a function of n, the expression of $\mu(n)$ is very complicated, which prevents us from obtaining analytical results for the dynamics of the system. A simple approach is to take a polytropic approximation, i.e., $\mu(n)\sim n^\gamma$,[18,23–30] with

$$\gamma = \gamma(\eta) = \frac{n}{\mu}\frac{\partial\mu}{\partial n} = \frac{\frac{2}{3}\sigma(\eta) - \frac{2\eta}{5}\sigma'(\eta) + \frac{\eta^2}{15}\sigma''(\eta)}{\sigma(\eta) - \frac{\eta}{5}\sigma'(\eta)}. \tag{3}$$

There are two well known limits for the value of the polytropic index γ. One is $\gamma=2/3$ at $\eta\to-\infty$ (BCS limit)[34] and another one is $\gamma=1$ at $\eta\to+\infty$ (BEC limit). The polytropic approximation has advantage of allowing one to obtain analytical results for various superfluid regimes in a unified way. In fact, polytropic approximation is quite accurate mathematically because γ is a slowly varying function of η and hence widely used in literature.[18,23–30]

Notice that in the superfluid state all fermions are paired with the superfluid density $n_s=n/2$ and superfluid velocity $\mathbf{v}_s=\mathbf{v}$, where $\mathbf{v}_s=(\hbar/M)\nabla\Phi_s$ with Φ_s being the phase of superfluid order parameter and $M=2m$ being the mass of fermionic pairs. With these superfluid variables, Eqs. (1a) and (1b) can be converted into the form

$$\frac{\partial n_s}{\partial t} + \nabla\cdot(n_s\mathbf{v}_s) = 0, \tag{4a}$$

$$M\frac{\partial \mathbf{v}_s}{\partial t} + \nabla\left[\frac{1}{2}M\mathbf{v}_s^2 + \mu_s(n_s) + V_{\text{ext}}^s(\mathbf{r})\right] = 0, \tag{4b}$$

with $\mu_s(n_s)=2\mu(2n_s)$ and $V_{\text{ext}}^s(\mathbf{r})=2V_{\text{ext}}(\mathbf{r})$.

B. Ground state and linear collective excitations

We now consider the ground state and linear collective excitations of a fermionic condensate based on the superfluid hydrodynamic equations (4a) and (4b). The ground state of the system corresponds to $\partial n_s/\partial t=0$ and $\mathbf{v}_s=0$. Assume $\mu_s(n_s)=\mu_0(n_s/n_0)^\gamma$, where μ_0 and n_0 are, respectively, reference chemical potential and pair density, introduced here for the convenience of later calculation. From Eq. (4), we obtain the Thomas–Fermi ground state pair density $n_{sG}(\mathbf{r})=n_0\{[\mu_G - V_{\text{ext}}^s(\mathbf{r})]/\mu_0\}^{1/\gamma}$ if $V_{\text{ext}}^s(\mathbf{r})<\mu_G$ and zero otherwise. Here, μ_G is ground state chemical potential. For the harmonic trapping potential,

$$V_{\text{ext}}^s(\mathbf{r}) = \frac{M}{2}(\omega_x^2x^2 + \omega_y^2y^2 + \omega_z^2z^2), \tag{5}$$

where ω_j is the trapping frequency in the jth ($j=x,y,z$) direction, and by the normalized condition $\int d\mathbf{r}n_{sG}(\mathbf{r})=N$, we obtain $\mu_G=(N/G_0)^{2\gamma/(3\gamma+2)}$. Here, $G_0=2\pi n_0B(3/2,1/\gamma+1)(8/M^3\omega_x^2\omega_y^2\omega_z^2)^{1/2}/\mu_0^{1/\gamma}$ and $B(3/2,1/\gamma+1)$ is beta function. Then, the ground state pair density can be expressed as

$$n_{sG}(\mathbf{r}) = \frac{N}{2\pi B\left(\frac{3}{2},\frac{1}{\gamma}+1\right)R_xR_yR_z}\left[1-\left(\frac{x}{R_x}\right)^2-\left(\frac{y}{R_y}\right)^2 - \left(\frac{z}{R_z}\right)^2\right]^{1/\gamma}, \tag{6}$$

where $R_j=[2\mu_G/(M\omega_j^2)]^{1/2}$ is the characteristic radius of the condensate in the jth direction.

The shape oscillation of the condensate can be described by assuming the time-dependent pair density

$$n_s(\mathbf{r},t) = \frac{N}{2\pi B\left(\frac{3}{2},\frac{1}{\gamma}+1\right)R_x(t)R_y(t)R_z(t)}\left\{1-\left[\frac{x}{R_x(t)}\right]^2 - \left[\frac{y}{R_y(t)}\right]^2-\left[\frac{z}{R_z(t)}\right]^2\right\}^{1/\gamma}, \tag{7}$$

with $R_j(t)=R_jb_j(t)$ and $[x_j/R_j(t)]^2\leqslant 1$. To fulfill the hydrody-

namic equations (4a) and (4b), one can set[31] $\mathbf{v}_s(\mathbf{r},t)=(1/2)\nabla[\alpha_x(t)x^2+\alpha_y(t)y^2+\alpha_z(t)z^2]$ with the initial condition $b_j(0)=1$, $\mathbf{v}_s(\mathbf{r},0)=0$, and $\alpha_j(0)=0$. Then, it is easy to show that the dimensionless spatial width of the condensate $b_j(t)$ satisfies the nonlinear dynamical equation

$$\frac{d^2b_j}{dt^2}+\omega_j^2 b_j-\frac{\omega_j^2}{b_j(b_xb_yb_z)^\gamma}=0, \tag{8}$$

with $\alpha_j=(db_j/dt)/b_j(j=x,y,z)$. Equation (8) controls the linear and nonlinear dynamics of the collective excitations in the system. The second term of Eq. (10) comes from the trapping potential, while the third one originates from the interaction between the fermionic atom pairs.

For an axial symmetric trap with anisotropic parameter $\lambda=\omega_z/\omega_\perp$ ($\omega_\perp=\omega_x=\omega_y$), Eq. (8) is converted into the simple form

$$\frac{d^2b_j}{d\tau^2}+\Delta_{jz}b_j-\frac{\Delta_{jz}}{b_j(b_xb_yb_z)^\gamma}=0, \tag{9}$$

where $\tau=\omega_\perp t$ and $\Delta_{jz}=[1+(\lambda^2-1)\delta_{jz}]$, with δ_{jz} being Kronecker symbol.

The linear excitations of the system can be obtained by assuming that $b_j(\tau)-1$ are much less than unity and proportional to constant$\times\exp(i\tilde{\omega}\tau)$+c.c., where c.c. represents complex conjugate. Then, by solving Eq. (9), one obtains readily the following three eigenvalues:[16–18]

$$\tilde{\omega}_2\equiv\frac{\omega_2}{\omega_\perp}=\sqrt{2}, \tag{10a}$$

$$\tilde{\omega}_\pm\equiv\frac{\omega_\pm}{\omega_\perp}=\left[\gamma+1+\left(\frac{\gamma}{2}+1\right)\lambda^2\pm\frac{1}{2}\sqrt{\Pi}\right]^{1/2}, \tag{10b}$$

where $\Pi=(\gamma+2)^2\lambda^4+4(\gamma^2-3\gamma-2)\lambda^2+4(\gamma+1)^2$. The corresponding eigenvectors are, respectively, given by

$$\mathbf{U}_2=(1,-1,0), \tag{11a}$$

$$\mathbf{U}_\pm=(1,1,V_\pm), \tag{11b}$$

with

$$V_\pm=(\tilde{\omega}_\pm^2-2\gamma-2)/\gamma. \tag{12}$$

The eigenvector $\mathbf{U}_2$, called $m=2$ mode, describes an oscillation that has no motion in z direction. It is a quadrupole-type excitation in the radial (i.e., x and y) directions corresponding to $(n,l,m)=(0,2,\pm2)$, where n, l, and m are, respectively, principal, angular momentum, and z component of the angular-momentum quantum numbers when expressing the eigenoscillation by spherical coordinates. The eigenvector $\mathbf{U}_+$ is called high-lying $m=0$ mode [corresponding to $(n,l,m)=(1,2,0)$], describing an in-phase oscillation along all directions; while the eigenvector $\mathbf{U}_-$, called low-lying $m=0$ mode [corresponds to $(n,l,m)=(1,0,0)$], describing an oscillation in the z direction that is out of phase with the oscillation in x and y directions.[23–27,30]

Figure 1(a) shows the eigenfrequencies of the high-lying and low-lying $m=0$ modes as functions of $1/(k_Fa_s)$ and λ. For clearness and for a comparison with well-known results,

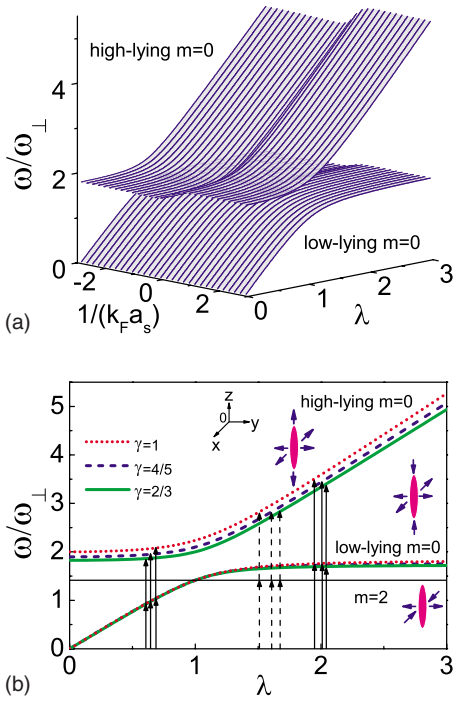

FIG. 1. (Color online) (a) Eigenfrequency $\omega/\omega_\perp$ of the high-lying and low-lying $m=0$ modes as functions of λ and $1/(k_Fa_s)$. (b) The upper (lower) curves represent the high-lying (low-lying) $m=0$ mode for different γ. The solid horizontal straight line is the frequency of $m=2$ mode. The solid and dashed vertical straight lines with arrows indicate the positions where second-harmonic generation processes may occur (for details, see text). The insets in (b) show the oscillating patterns of the $m=2$ mode, the high-lying $m=0$ mode, and the low-lying $m=0$ mode, respectively.

a two-dimensional cross-section diagram of the eigenfrequencies as functions of λ is shown in Fig. 1(b) for several different values of γ. The horizontal straight line is the frequency of the $m=2$ mode (i.e., $\omega/\omega_\perp=\sqrt{2}$). The result for $\gamma=1$ corresponds to the BEC limit, which was first obtained theoretically by Stringari[35] and lately observed in many experiments.[36–38] From the figure, we see that the eigenfrequencies of the high-lying and low-lying $m=0$ modes depend strongly on the trapping parameter λ. However, they are not sensitive to the change of the polytropic index γ. However, we shall show in the next section that frequency corrections due to the nonlinear effect as functions of γ [or $1/(k_Fa_s)$] are significant when passing through the BCS-BEC crossover.

In Fig. 1(b), we have shown by solid vertical straight lines with arrows the positions where a second-harmonic generation phase-matching condition (i.e., $\tilde{\omega}_+=2\tilde{\omega}_-$) can be satisfied, which is given by $\lambda=(15\sqrt{2}\pm\sqrt{130})/16$ for $\gamma=2/3$, $\lambda=(5\sqrt{55}\pm\sqrt{367})/28$ for $\gamma=4/5$, and $\lambda=(5\sqrt{10}\pm\sqrt{58})/12$ for $\gamma=1$. We have also shown by the dashed vertical straight lines with arrows the positions for additional second-harmonic generation phase-matching condition, i.e., $\tilde{\omega}_+=2\tilde{\omega}_2$, which is given by $\lambda=\sqrt{70}/5$ for $\gamma=2/3$, $\lambda=2\sqrt{187}/17$ for $\gamma=4/5$, and $\lambda=4\sqrt{7}/7$ for $\gamma=1$, respectively.

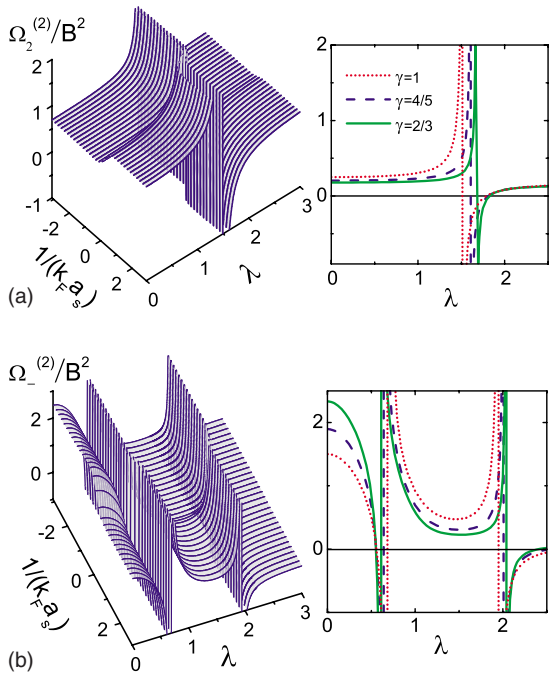

FIG. 2. (Color online) The second-order frequency shifts of $\Omega_2^{(2)}$ (a) for the $m=2$ mode and $\Omega_-^{(2)}$ (b) for the low-lying $m=0$ mode as functions of λ and $1/(k_F a_s)$. The vertical lines in the two-dimensional cross-section diagram on the right hand side of each panel are the positions where a second-harmonic generation occurs.

III. NONLINEAR FREQUENCY SHIFT OF THE COLLECTIVE MODES

We are interested in the nonlinear dynamics of the collective modes. We assume that the external perturbation for generating the collective modes is not too large, so that the nonlinear response of the system is weak. In this case, one can apply a weak nonlinear theory to calculate the nonlinear frequency shift and resonant mode coupling of the collective modes. We consider first the frequency shift due to a large amplitude excitation. In order to get the frequency shift in a systematic way, we apply the standard singular perturbation method due to Lindstedt and Poincaré.[39] Introducing a new dimensionless time variable $T=\Omega\omega_\perp t$ and making the asymptotic expansion

$$\Omega = 1 + \varepsilon\Omega^{(1)} + \varepsilon^2\Omega^{(2)} + \varepsilon^3\Omega^{(3)} + \cdots, \tag{13a}$$

$$b_j = 1 + j^{(1)} + \varepsilon^2 b_j^{(2)} + \varepsilon^3 b_j^{(3)} + \cdots, \quad (j = x,y,z), \tag{13b}$$

where ε is a small parameter representing the amplitude of the excitation, Eq. (8) is converted into the form

$$\frac{d^2}{dT^2}\begin{pmatrix} b_x^{(n)} \\ b_y^{(n)} \\ b_z^{(n)} \end{pmatrix} + \begin{pmatrix} \gamma+2 & \gamma & \gamma \\ \gamma & \gamma+2 & \gamma \\ \lambda^2\gamma & \lambda^2\gamma & \lambda^2(\gamma+2) \end{pmatrix}\begin{pmatrix} b_x^{(n)} \\ b_y^{(n)} \\ b_z^{(n)} \end{pmatrix} = \begin{pmatrix} f_x^{(n)} \\ f_y^{(n)} \\ f_z^{(n)} \end{pmatrix}, \tag{14}$$

where the explicit expressions of $f_j^{(n)}$ $(n=1,2,3,\ldots)$ are omitted for saving space.

The above equations can be rewritten as

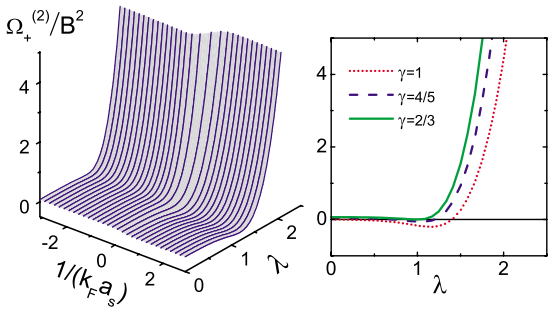

FIG. 3. (Color online) The second-order frequency shift $\Omega_+^{(2)}$ of the high-lying $m=0$ mode as a function of λ and γ.

$$\hat{\mathcal{L}} b_x^{(n)} = \mathcal{S}^{(n)}, \tag{15a}$$

$$b_y^{(n)} = \frac{1}{\gamma}[-(D^2+\gamma+2)b_x^{(n)} - \gamma b_z^{(n)} + f_x^{(n)}], \tag{15b}$$

$$b_z^{(n)} = (D^2+2\lambda^2)^{-1}[(D^2+2)\lambda^2 b_x^{(n)} - \lambda^2 f_x^{(n)} + f_z^{(n)}], \tag{15c}$$

where

$$\hat{\mathcal{L}} = D^6 + (\gamma+2)(\lambda^2+2)D^4 + 4(\gamma+1)(2\lambda^2+1)D^2 + 4(3\gamma+2)\lambda^2, \tag{16}$$

$$\mathcal{S}^{(n)} = [D^4 + (\gamma+2)(\lambda^2+1)D^2 + 4(\gamma+1)\lambda^2]f_x^{(n)} - \gamma(D^2+2\lambda^2)f_y^{(n)} - \gamma(D^2+2)f_z^{(n)}, \tag{17}$$

with $D=d/dT$. One can solve $b_x^{(n)}$ from Eq. (15a) and then get $b_y^{(n)}$ and $b_z^{(n)}$ from Eqs. (15b) and (15c), respectively.

At the leading order $(n=1)$, one has $\mathcal{S}^{(1)}=0$. The solution of Eq. (15a) reads

$$b_x^{(1)} = \frac{B}{2}e^{-i\tilde{\omega}T} + \text{c.c.}, \tag{18}$$

where B is a constant. One of the eigenfrequencies is $\tilde{\omega}=\tilde{\omega}_2$ (i.e., the $m=2$ mode). In this case, by solving Eqs. (15b) and (15c), we have $b_y^{(1)}=-b_x^{(1)}$ and $b_z^{(1)}=0$. The other two eigenfrequencies are given by $\tilde{\omega}=\tilde{\omega}_\pm$ (i.e., the high-lying and low-lying $m=0$ modes) with $b_y^{(1)}=b_x^{(1)}$ and $b_z^{(1)}=V_\pm b_x^{(1)}$. The property of such eigensolutions has been discussed in the last section.

We first consider the nonlinear frequency shift for the $m=2$ mode. By using the first-order solution given above, one can obtain $\mathcal{S}^{(2)}$. The second-order equation for the $m=2$ mode reads

$$\hat{\mathcal{L}} b_x^{(2)} = \left(\frac{3\gamma}{2}+1\right)\lambda^2 B^2 + 8\Omega^{(1)}\gamma(\lambda^2-1)Be^{-i\sqrt{2}T} + \left[12(\gamma+1) - \left(\frac{9\gamma}{2}+3\right)\lambda^2\right]B^2 e^{-i2\sqrt{2}T} + \text{c.c.} \tag{19}$$

Notice that $\exp(-i\sqrt{2}T)$ is the eigenfunction of the operator

$\hat{\mathcal{L}}$, so the second term on the right hand side of Eq. (19) is a secular one. Such secular term must be eliminated in order to make the second-order solution be divergence-free. Thus, we obtain the condition of eliminating the secular term, $\Omega^{(1)}=0$, i.e., the first-order frequency shift is zero. Then, one can get the explicit expression of divergence-free second-order solution $b_j^{(2)}$ $(j=x,y,z)$ by Eq. (26) and Eqs. (15b) and (15c) for $n=2$, which is omitted here for saving space.

At the third order $(n=3)$, we have

$$\mathcal{L}b_x^{(3)} = 8\gamma(\lambda^2-1)\left[\Omega_2^{(2)} - \frac{(3\gamma+2)\lambda^2-8(\gamma+1)}{4[(\gamma+6)\lambda^2+8(\gamma-3)]}B^2\right]Be^{-i\sqrt{2}T} + \text{nonsecular terms} + \text{c.c.} \tag{20}$$

Obviously, the requirement of eliminating the secular term in the above equation results in the second-order frequency shift

$$\Omega_2^{(2)}(\gamma,\lambda) = \frac{(3\gamma+2)\lambda^2-8(\gamma+1)}{4[(\gamma+6)\lambda^2+8(\gamma-3)]}B^2. \tag{21}$$

When $\gamma=1$, this general expression recovers the result for the BEC limit, first found by Dalfovo *et al.*[31]

In a similar way, we can calculate the nonlinear frequency shifts of the high-lying and low-lying $m=0$ modes. We found that their first-order frequency shifts are also zero. The second-order frequency shifts are given by

$$\Omega_\pm^{(2)}(\gamma,\lambda) = \frac{d_1+d_2+d_3}{16d_4\{[2(2+\gamma)\tilde{\omega}_\pm^2-(3\gamma+2)]\lambda^2-4\tilde{\omega}_\pm^2(2\tilde{\omega}_\pm^2-\gamma-1)\}}B^2. \tag{22}$$

The detailed expressions of d_j $(j=1-4)$ are listed in Appendix A.

From the results (21) and (22), we obtain the dimensional oscillating frequencies of the collective modes up to the second-order corrections

$$\omega_\alpha^{\text{col}} = \omega_\perp\tilde{\omega}_\alpha[1+B^2\Omega_\alpha^{(2)}(\gamma,\lambda)], \tag{23}$$

where $\alpha=2$ is for the $m=2$ mode and $\alpha=+$ $(\alpha=-)$ for the high-lying (low-lying) $m=0$ mode.

Because $\Omega_\alpha^{(2)}$ are functions of the trapping parameters λ and the polytropic index γ, the frequency corrections due to the nonlinear effect display different features for different λ and γ. For illustration, we have shown the frequency shifts $\Omega_\alpha^{(2)}$ as functions of λ and $1/(k_Fa_s)$ in Figs. 2 and 3. For a comparison with the work by Dalfovo *et al.*,[31] the corresponding cross-section diagrams for several different γ values (i.e., $\gamma=1$, $4/5$, $2/3$) are also shown. We see that the frequency shifts possess many interesting features and have very strong dependence on the trapping parameters λ and the interaction parameter $1/(k_Fa_s)$. First, for the $m=2$ mode and low-lying $m=0$ mode, the frequency shifts display divergence behaviors for some λ values (see Fig. 2), which correspond to the appearance of the SHG. In this case, the perturbation expansions (13a) and (13b) are not valid anymore and we must seek a new expansion to solve the nonlinear dynamical equation (8). Such situation will be investigated in detail in the next section. Second, in different superfluid regimes, the positions for the SHG are different. For example, for the $m=2$ mode, the SHG occurs at $\lambda=\sqrt{70}/5$ $(\lambda=4\sqrt{7}/7)$ for the BCS (BEC) limit, while for the low-lying $m=0$ mode the SHG happens at $\lambda=15\sqrt{2}\pm\sqrt{130})/16$ $[\lambda=(5\sqrt{10}\pm\sqrt{58})/12]$ for the BCS (BEC) limit, as indicated already in Fig. 1. Third, the frequency shifts may be positive, zero, and negative, relying on the values of λ and γ. Finally, the result presented here recovers the special result obtained by Dalfovo *et al.*,[31] for a condensed Bose gas $(\gamma=1)$.

In order to understand more clearly the transition behavior of the nonlinear frequency shifts in the whole BCS-BEC crossover, in Fig. 4 we have shown $\Omega_\alpha^{(2)}$ $(\alpha=2,\pm)$ as functions of the interaction parameter $1/(k_Fa_s)$ by choosing several different λ values. We see that depending on λ, the frequency shifts have very different properties when passing from the BCS regime to the BEC regime. (i) For the $m=2$ mode (the upper panel), the frequency shift is generally higher in the BEC regime than in the BCS regime; while for the high-lying $m=0$ mode (the middle panel), the behavior is reversed. (ii) The frequency shift for the low-lying $m=0$ mode (the lower panel) is very complicated. It may be larger or smaller in the BCS regime than in the BEC regime, depending on the value of λ.

Figure 5 shows the dependence of the collective-mode frequencies on the parameter B (i.e., the amplitude of the collective modes) for $\lambda=0.1$ and several different values of γ. One can see that as B increases, the oscillating frequency of the $m=2$ mode (the upper panel) increases quadratically, with its value being smaller in the BCS limit than in the BEC limit. However, the oscillating frequencies for both the high-lying (the middle panel) and the low-lying (the lower panel) $m=0$ modes are higher in the BCS limit than in the BEC limit. In particular, the oscillating frequency of the high-lying $m=0$ mode in the BEC limit is nearly independent of the amplitude B (i.e., the horizontal straight line in the middle panel).

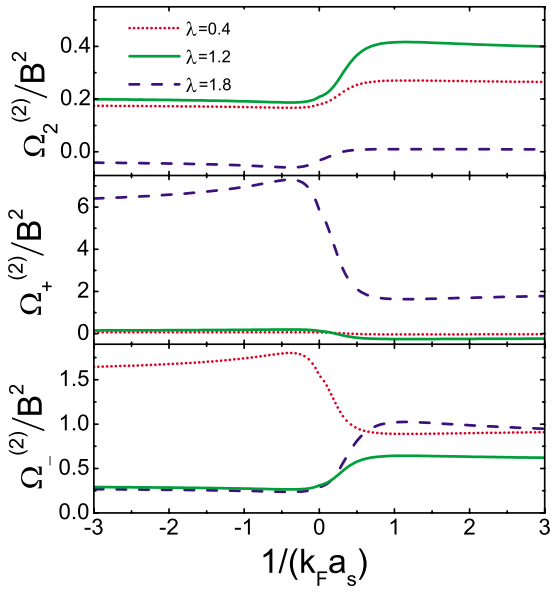

FIG. 4. (Color online) Frequency shifts $\Omega_2^{(2)}$ (upper panel), $\Omega_+^{(2)}$ (middle panel), and $\Omega_-^{(2)}$ (lower panel) as functions of the interaction parameter $1/(k_F a_s)$ for several different values of the trapping parameter λ.

IV. MODE COUPLING OF THE SUPERFLUID FERMI GAS

A. Envelope equations and their solutions for second-harmonic generation

We now investigate the resonant mode coupling due to the nonlinear interaction between the collective modes of the system. As indicated in the last section, the divergences that appeared in the expressions of the second-order frequency shifts $\Omega_\alpha^{(2)}$ are the signature of second harmonic generation. In this situation, the asymptotic expansions (13a) and (13b) are not valid anymore and one must find a new asymptotic expansion to solve the nonlinear dynamic equation (8) and (9) to obtain the solutions of second harmonic generation.

We apply the method of multiple scales[39,40] to study the second harmonic generation in the system. We assume $b_j = 1 + j^{(1)} + \varepsilon^2 b_j^{(2)} + \cdots$, where $b_j^{(n)}$ $(j=x,y,z)$ are the functions of τ and $\tau_1 = \varepsilon\tau$ with τ_1 being a slow variable characterizing the time evolution of the envelopes of the collective modes. Since τ and τ_1 are taken as independent variables, we have the derivative transformation $\mathrm{d}/\mathrm{d}\tau = D_0 + \varepsilon D_1$ with $D_0 = \partial/\partial\tau$ and $D_1 = \partial/\partial\tau_1$.[39,40] With these considerations, Eq. (9) becomes

$$\hat{\mathcal{L}}_1 b_x^{(n)} = \mathcal{P}^{(n)}, \tag{24a}$$

$$b_y^{(n)} = \frac{1}{\gamma}[-(D_0^2 + \gamma + 2)b_x^{(n)} - \gamma b_z^{(n)} + g_x^{(n)}], \tag{24b}$$

$$b_z^{(n)} = (D_0^2 + 2\lambda^2)^{-1}[(D_0^2 + 2)\lambda^2 b_x^{(n)} - \lambda^2 g_x^{(n)} + g_z^{(n)}], \tag{24c}$$

with

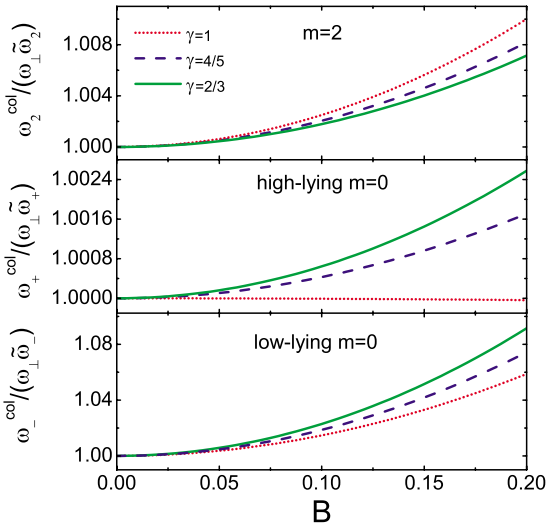

FIG. 5. (Color online) Dimensionless oscillating frequencies $\omega_\alpha^{\mathrm{col}}/(\omega_\perp \tilde{\omega}_\alpha)$ $(\alpha = 2, \pm)$ of the $m=2$ mode (upper panel), and the high-lying (middle panel) and the low-lying (lower panel) $m=0$ modes for $\lambda = 0.1$ and several different γ values.

$$\hat{\mathcal{L}}_1 = D_0^6 + (\gamma+2)(\lambda^2+2)D_0^4 + 4(\gamma+1)(2\lambda^2+1)D_0^2 + 4(3\gamma + 2)\lambda^2, \tag{25}$$

$$\mathcal{P}^{(n)} = [D_0^4 + (\gamma+2)(\lambda^2+1)D_0^2 + 4(\gamma+1)\lambda^2]g_x^{(n)} - \gamma(D_0^2 + 2\lambda^2)g_y^{(n)} - \gamma(D_0^2+2)g_z^{(n)}. \tag{26}$$

The expressions for $g_j^{(n)}$ $(n=1,2$ and $j=x,y,z)$ are given by

$$g_j^{(1)} = 0, \tag{27}$$

$$g_j^{(2)} = -2D_0 D_1 b_j^{(1)} + \Delta_{jz}\left\{ b_j^{(1)2} - \gamma(b_x^{(1)}b_y^{(1)} + b_y^{(1)}b_z^{(1)} + b_z^{(1)}b_x^{(1)}) + \frac{\gamma}{2}(b_x^{(1)} + b_y^{(1)} + b_z^{(1)})[2b_j^{(1)} + (\gamma+1)(b_x^{(1)} + b_y^{(1)} + b_z^{(1)})] \right\}. \tag{28}$$

The leading-order solution of Eq. (24a) reads

$$b_x^{(1)} = \frac{B(\tau_1)}{2} e^{-i\tilde{\omega}\tau} + \text{c.c.}, \tag{29}$$

where B is an undetermined function and $\tilde{\omega} = \tilde{\omega}_\alpha$ $(\alpha = 2, \pm)$ are the eigenfrequencies of the collective modes, given by Eqs. (10a) and (10b). The expressions of $b_y^{(1)}$ and $b_z^{(1)}$ can be obtained by Eqs. (24b) and (24c).

From the discussion in the last two sections, we know that the system may have SHG, which means that even if only one eigenmode (as fundamental wave) is created initially, a new oscillating component (as second harmonic wave) will grow rapidly through an efficient energy transfer between the fundamental wave and the second-harmonic wave. This efficient energy transfer (i.e., resonant mode coupling) can be realized in various superfluid regimes under the phase-

matching condition that may be fulfilled by choosing appropriate values of λ and $1/(k_F a_s)$, as pointed out in the last paragraph of Sec. II.

We consider the second-harmonic generation between the high-lying and the low-lying $m=0$ modes. Because in the case of the SHG the fundamental wave and the second-harmonic wave have the same order of magnitude, we must take the leading-order solution as

$$b_x^{(1)} = \frac{B_-(\tau_1)}{2} e^{-i\tilde{\omega}_- \tau} + \frac{B_+(\tau_1)}{2} e^{-i\tilde{\omega}_+ \tau} + \text{c.c.}, \tag{30}$$

with the phase-matching condition $\tilde{\omega}_+ = 2\tilde{\omega}_-$, where B_+ and B_- are two functions yet to be determined.

Using the expression (30), we can calculate $\mathcal{P}^{(2)}$ explicitly. Then, by the conditions of eliminating the secular term in the second-order equation $\hat{\mathcal{L}}_1 b_x^{(2)} = \mathcal{P}^{(2)}$, we obtain

$$\frac{\partial B_-}{\partial \tau_1} = \frac{i}{2\tilde{\omega}_-} \frac{J_-}{I_-} B_-^* B_+, \tag{31a}$$

$$\frac{\partial B_+}{\partial \tau_1} = \frac{i}{2\tilde{\omega}_+} \frac{J_+}{I_+} B_-^2, \tag{31b}$$

where the expressions of $I_\pm$ and $J_\pm$ are given in Appendix B.

The solutions of Eqs. (31a) and (31b) are well known in nonlinear optics.[41] Let $B_- = [2\tilde{\omega}_+ I_+ W_0 / J_+]^{1/2} u \exp(-i\phi_1)$ and $B_+ = [2\tilde{\omega}_- I_- W_0 / J_-]^{1/2} v \exp(-i\phi_2)$; here, W_0 is a constant proportional to total initial input power of the collective mode and ϕ_1 and ϕ_2 are phase constants; Eqs. (31a) and (31b) become two coupled differential equations for u and v. It is easy to show that these equations possess two conservation laws $u^2 + v^2 = 1$ and $u^2 v \cos(\phi_2 - 2\phi_1) = C$ with C being a constant. For the case $C=0$, one has the solution

$$B_- = \left[\frac{2\tilde{\omega}_+ I_+ W_0}{J_+}\right]^{1/2} \operatorname{sech}\left[\left(\frac{J_- W_0}{2\tilde{\omega}_- I_-}\right)^{1/2} \tau_1\right] e^{i\phi_1}, \tag{32a}$$

$$B_+ = \left[\frac{2\tilde{\omega}_- I_- W_0}{J_-}\right]^{1/2} \tanh\left[\left(\frac{J_- W_0}{2\tilde{\omega}_- I_-}\right)^{1/2} \tau_1\right] e^{i(2\phi_1 + \pi/2)}, \tag{32b}$$

where ϕ_1 is an arbitrary constant. In the general case (i.e., $C \neq 0$), analytical solutions of Eqs. (31a) and (31b) with the form of Jacobian elliptic functions can also be obtained,[41] which are omitted here.

Shown in Fig. 6 are the results of the time evolution of the SHG for the case $C=0$ and the case $C=1/\sqrt{27}$ in the BCS-BEC crossover, respectively. We see that for both cases, the growth and descent of the second-harmonic component v is slower in the BCS regime ($\gamma=2/3$) than in the BEC regime ($\gamma=1$). Such SHG behavior should be observed experimentally in the superfluid Fermi gas. Note that a beautiful experiment for second-harmonic resonance between $\tilde{\omega}_+$ and $\tilde{\omega}_-$ in a condensed Bose gas (i.e., in the BEC limit) has been carried out by Hechenblaikner *et al.*[42]

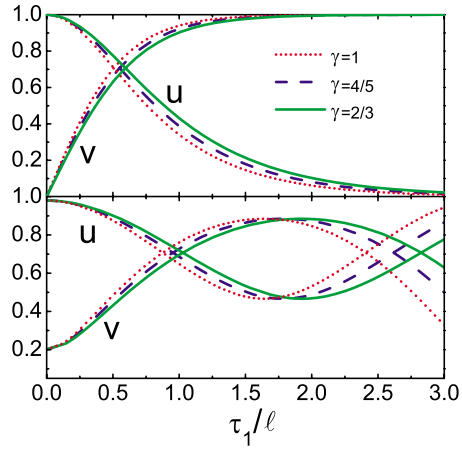

FIG. 6. (Color online) The time evolution of the second-harmonic generation between the high-lying and the low-lying $m=0$ modes for several different γ values. u (v) represents the fundamental (second-harmonic) wave as a function of τ_1/ℓ with $\ell = [2\tilde{\omega}_- I_- / (J_- W_0)]^{1/2}$. The upper panel is the case for $C=0$, while the lower panel is for $C=1/\sqrt{27}$.

We have also made a calculation on the second-harmonic generation between the $m=2$ mode and the high-lying $m=0$ mode (with the phase-matching condition $\omega_+ = 2\omega_2$). The result obtained is similar and thus omitted here.

B. Numerical study of the second-harmonic generation

In order to check the analytical prediction of the second-harmonic generation presented above, detailed numerical simulations are carried out based on the nonlinear dynamical equation (8), which describes the time evolution of the spatial widths of the fermionic condensate with the initial value $b_j(0)=1$. To obtain a significant SHG, the corresponding fundamental wave of large enough amplitude must be excited firstly. One can realize such process by modulating the trap frequencies ω_j ($j=x,y,z$) for a period of time and then let the system oscillate freely under the SHG phase-matching condition. The corresponding numerical simulation is to solve Eq. (8) by using time-dependent trapping frequencies with the form $\omega_j^2(t) = \omega_j^2[1 + 2k_j(t)]$, where $k_j(t)$ is an appropriate sinusoidal function within a finite time interval.

We assume $k_j(t)$ ($j=x,y,z$) take the form

$$k_x(t) = k_y(t) = A_\perp \theta(T_d - t) \sin \nu_d t, \tag{33a}$$

$$k_z(t) = A_z \theta(T_d - t) \sin \nu_d t, \tag{33b}$$

where θ is Heaviside step function, T_d is the drive time, and $A_\perp$ and A_z are drive amplitudes. The drive frequency is chosen as $\nu_d = \tilde{\omega}_- - \omega_\perp$, which is the eigenfrequency of the low-lying $m=0$ mode.

To obtain a significant SHG between the low-lying and the high-lying $m=0$ modes, the corresponding phase-matching condition ($\tilde{\omega}_+ = 2\tilde{\omega}_-$) must be satisfied. For instance, in the BCS (BEC) limit, the phase-matching condition is given by $\lambda = (15\sqrt{2} + \sqrt{130})/16$ [$\lambda = (5\sqrt{10} + \sqrt{58})/12$] (see the last paragraph of Sec. II). We have made a series of

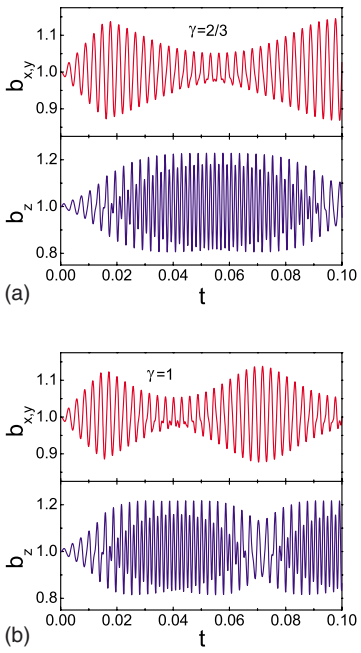

FIG. 7. (Color online) The numerical result of the time evolution for the spatial widths of the fermionic condensate in the case of the second-harmonic generation between the low-lying and the high-lying $m=0$ modes. (a) and (b) are the time evolution of $b_j(t)$ $(j=x,y,z)$ in the BCS $(\gamma=2/3)$ and BEC $(\gamma=1)$ limits, respectively. The second-harmonic generation occurs significantly in the width oscillation of the z direction.

numerical simulation for the SHG in different superfluid regimes. Here, we just present the results in the BCS and BEC limits.

We choose the radial trapping frequency $\omega_\perp=400\pi$ Hz and the drive parameters $A_\perp=0.01$ and $A_z=-0.007$. Under such drive condition, the fundamental wave (i.e., the low-lying $m=0$ mode) can be excited to a large enough amplitude. We switch off the drive at time $T_d=20\omega_\perp^{-1}=0.016$ s and then let the system oscillate freely. Due to the nonlinear effect of the system, a second-harmonic wave (i.e., the high-lying $m=0$ mode) is generated and grow rapidly due to the nonlinear effect of the system.

Shown in Fig. 7 is the result of the numerical simulation for the SHG between the low-lying and the high-lying $m=0$ modes. Panels (a) and (b) are the time evolution of $b_j(t)$ $(j=x,y,z)$ in the BCS $(\gamma=2/3)$ and BEC $(\gamma=1)$ limits, respectively. We see clearly that the second-harmonic generation occurs significantly in the width oscillation of the axial (i.e., z) direction. In the radial (i.e., x and y) directions, one can also find a signature of the SHG but it is much smaller in comparison with that in the axial direction. The physical reason for the anisotropic behavior of the SHG is that the coupling coefficient between the fundamental wave and the second-harmonic wave in the radial directions is much weaker than that in the axial direction, though the phase-matching condition is fulfilled. Consequently, if one explores the SHG between the low-lying and the high-lying $m=0$ modes by observing the oscillation of the spatial width of the fermionic condensate, the experimental measurement should be chosen along the axial direction, where the SHG signature is stronger. Note that such strong anisotropic SHG of the collective modes for the condensed bosonic atoms (i.e., ^{87}Rb) in a harmonic trap has been observed by Hechenblaikner *et al.*[42]

The results of Fig. 7 show also that there are obvious differences of the second-harmonic generation in different superfluid regimes. One of them is that for different γ, there are different periods of the energy transfer between the fundamental wave and the second-harmonic wave. For $\gamma=2/3$ (i.e., BCS limit), the period of the energy transfer in the SHG process is 0.07 s; while for $\gamma=1$ (BEC limit), the period of the energy transfer of the SHG is only 0.05 s. All numerical simulations presented above agree well with the analytical results given in the last section.

V. SUMMARY

We have investigated the nonlinear dynamical behavior of the collective modes in a superfluid Fermi gas in the BCS-BEC crossover based on a simple hydrodynamic approach. We have solved the superfluid hydrodynamic equations governing the time evolution of the fermionic condensate in the BCS-BEC crossover by using standard singular perturbation methods. In particular, we have calculated the frequency shifts of the collective modes induced by nonlinear effects by using the Lindstedt–Poincaré method. The results obtained demonstrate that the frequency shifts possess different features in different superfluid regimes. Especially, the frequency shifts may be positive, zero, and negative, depending on the values of the polytropic index γ of the state equation and the anisotropic parameters λ of the trapping potential. For the $m=2$ mode, the frequency shift is generally higher in the BEC regime than in the BCS regime, but for the high-lying $m=0$ mode the behavior is reversed. The frequency shift for the low-lying $m=0$ mode has a very complicated behavior, which may be larger or smaller in the BCS regime than in the BEC regime, depending on the value of λ. Generally speaking, for all collective modes and in various superfluid regimes, the frequency shifts increase quadratically as functions of the mode amplitudes. Furthermore, the divergent points of the frequency shifts obtained determine the positions of the second-harmonic generation, which are also the functions of γ and λ. In addition, we have studied in detail the second-harmonic generation of the collective modes under phase-matching conditions both analytically and numerically, and obvious difference for the SHG in different superfluid regimes is found. In particular, we have found that the growth and descent of the second-harmonic component is slower in the BCS regime than in the BEC regime, and the period of the energy transfer of the SHG in the BCS regime is obviously larger than that in the BEC regime. Such behavior of the second-harmonic generation should be observed experimentally in the superfluid Fermi gas. The results presented in this work may be useful for understanding the nonlinear property of fermionic condensates in the BCS-BEC crossover and guiding the experimental findings of the frequency shifts and mode couplings in ultracold quantum degenerate Fermi atomic gases.

ACKNOWLEDGMENTS

This work was supported by NSF-China under Grants Nos. 10434060 and 10674060, by the Key Development Program for Basic Research of China under Grants Nos. 2005CB724508 and 2006CB921104, by the Program for Changjiang Scholars and Innovative Research Team of Chinese Ministry of Education, and by the Ph.D. Program Scholarship Fund of ECNU 2007.

APPENDIX A: EXPRESSIONS OF d_j

Parameters d_j $(j=1-4)$ in Eq. (22) read

$$d_1 = 2(\gamma+1)(\gamma+2)^2\tilde{\omega}_{\pm}^8 + (3\gamma+2)[(\gamma+2)(4\gamma^2-13\gamma - 13)\tilde{\omega}_{\pm}^6 - (21\gamma^3-52\gamma^2-150\gamma-60)\tilde{\omega}_{\pm}^4 - (3\gamma^3+154\gamma^2 + 196\gamma+56)\tilde{\omega}_{\pm}^2 + 2(\gamma+2)(5\gamma+2)(3\gamma+2)], \quad \text{(A1a)}$$

$$d_2 = -2(2\gamma+5)(\gamma+1)(\gamma+2)\tilde{\omega}_{\pm}^{10} + (40\gamma^3+327\gamma^2+397\gamma + 130)\tilde{\omega}_{\pm}^8 - (3\gamma+2)(169\gamma^2+404\gamma+150)\tilde{\omega}_{\pm}^6 + (3\gamma+2) \times(102\gamma^3+483\gamma^2+532\gamma+140)\tilde{\omega}_{\pm}^4 - 2(3\gamma+2)(\gamma+1) \times(57\gamma^2+76\gamma+20)\tilde{\omega}_{\pm}^2, \quad \text{(A1b)}$$

$$d_3 = 8\gamma(\gamma+1)\tilde{\omega}_{\pm}^{12} - 2\gamma(4\gamma^2+43\gamma+31)\tilde{\omega}_{\pm}^{10} + 4\gamma(27\gamma^2+79\gamma + 41)\tilde{\omega}^8 - 4\gamma(4\gamma+21)(3\gamma+2)(\gamma+1)\tilde{\omega}_{\pm}^6 + 24\gamma(3\gamma+2) \times(\gamma+1)^2\tilde{\omega}_{\pm}^4, \quad \text{(A1c)}$$

$$d_4 = (-2\tilde{\omega}_{\pm}^2 + \gamma\lambda^2 + 2\lambda^2 + 2\gamma + 2)\gamma^2\tilde{\omega}_{\pm}^2, \quad \text{(A1d)}$$

where $\tilde{\omega}_{\pm}$ have been given by Eq. (10b).

APPENDIX B: COEFFICIENTS OF EQUATIONS (31a) and (31b)

The coefficients of Eqs. (31a) and (31b) are

$$I_{\pm} = a_{\pm} + b_{\pm} + c_{\pm}V_{\pm}, \quad \text{(B1)}$$

$$J_{\pm} = (a_{\pm} + b_{\pm})P_{\pm} + c_{\pm}\lambda^2 Q_{\pm}, \quad \text{(B2)}$$

with

$$a_{\pm} = \tilde{\omega}_{\pm}^4 - (\gamma+2)(\lambda^2+1)\tilde{\omega}_{\pm}^2 + 4(\gamma+1)\lambda^2,$$

$$b_{\pm} = -\gamma(-\tilde{\omega}_{\pm}^2 + 2\lambda^2),$$

$$c_{\pm} = -\gamma(-\tilde{\omega}_{\pm}^2 + 2),$$

$$P_+ = 1 - \gamma(1+2V_-) + \frac{\gamma}{2}(2+V_-)[2+(\gamma+1)(2+V_-)],$$

$$P_- = 2 + \gamma[2 - V_- - V_+ + (\gamma+1)(2+V_-)(2+V_+)],$$

$$Q_+ = V_-^2 - \gamma(1+2V_-) + \frac{\gamma}{2}(2+V_-)[2V_- + (\gamma+1)(2+V_-)],$$

$$Q_- = 2V_-V_+ - 2\gamma(1+V_-+V_+) + \gamma[2V_- + 2V_+ + 2V_-V_+ + (\gamma + 1)(2+V_-)(2+V_+)],$$

where $V_{\pm}$ have been given by Eq. (12).

*gxhuang@phy.ecnu.edu.cn

[1] M. Randeria, in *Bose Einstein Condensation*, edited by A. Griffin, D. W. Snoke, and S. Stringari (Cambridge University Press, Cambridge, 1995), p. 355.

[2] Q. Chen, J. Stajic, S. Tan, and K. Levin, Phys. Rep. **412**, 1 (2005).

[3] A. J. Leggett, *Quantum Liquids* (Oxford University Press, New York, 2006).

[4] S. Giorgini, L. P. Pitaevskii, and S. Stringari, arXiv:0706.3360 Rev. Mod. Phys. (to be published).

[5] B. DeMacro and D. S. Jin, Science **285**, 1703 (1999); K. M. O'Hara, S. R. Granade, M. E. Gehm, T. A. Savard, S. Bali, C. Freed, and J. E. Thomas, Phys. Rev. Lett. **82**, 4204 (1999); A. G. Truscott, K. E. Strecker, W. I. McAlexander, G. B. Partridge, and R. G. Hulet, Science **291**, 2570 (2001); T. Fukuhara, Y. Takasu, M. Kumakura, and Y. Takahashi, Phys. Rev. Lett. **98**, 030401 (2007).

[6] S. Jochim, M. Bartenstein, A. Altmeyer, G. Hendl, S. Riedl, C. Chin, J. H. Denschlag, and R. Grimm, Science **302**, 2101 (2003); M. Greiner, C. A. Regal, and D. S. Jin, Nature (London) **426**, 537 (2003); M. W. Zwierlein, C. A. Stan, C. H. Schunck, S. M. F. Raupach, S. Gupta, Z. Hadzibabic, and W. Ketterle, Phys. Rev. Lett. **91**, 250401 (2003).

[7] C. Chin, M. Bartenstein, A. Altmeyer, S. Riedl, S. Jochim, J. H. Denschlag, and R. Grimm, Science **305**, 1128 (2004).

[8] C. A. Regal, M. Greiner, and D. S. Jin, Phys. Rev. Lett. **92**, 040403 (2004); M. W. Zwierlein, C. A. Stan, C. H. Schunck, S. M. F. Raupach, A. J. Kerman, and W. Ketterle, *ibid.* **92**, 120403 (2004).

[9] M. Bartenstein, A. Altmeyer, S. Riedl, S. Jochim, C. Chin, J. H. Denschlag, and R. Grimm, Phys. Rev. Lett. **92**, 203201 (2004).

[10] J. Kinast, S. L. Hemmer, M. E. Gehm, A. Turlapov, and J. E. Thomas, Phys. Rev. Lett. **92**, 150402 (2004); J. Kinast, A. Turlapov, and J. E. Thomas, Phys. Rev. A **70**, 051401(R) (2004); Phys. Rev. Lett. **94**, 170404 (2005).

[11] M. Greiner, C. A. Regal, and D. S. Jin, Phys. Rev. Lett. **94**, 070403 (2005).

[12] A. Altmeyer, S. Riedl, C. Kohstall, M. J. Wright, R. Geursen, M. Bartenstein, C. Chin, J. H. Denschlag, and R. Grimm, Phys. Rev. Lett. **98**, 040401 (2007); M. J. Wright, S. Riedl, A. Altmeyer, C. Kohstall, E. R. S. Guajardo, J. H. Denschlag, and R. Grimm, *ibid.* **99**, 150403 (2007); A. Altmeyer, S. Riedl, M. J. Wright, C. Kohstall, J. H. Denschlag, and R. Grimm, Phys. Rev. A **76**, 033610 (2007).

[13] R. Grimm, in *Proceedings of the International School of Physics "Enrico Fermi*," Course CLXIV, Varenna, 20–30 June 2006, edited by M. Inguscio, W. Ketterle, and C. Salomon, arXiv:cond-mat/0703091 (to be published).
[14] J. Joseph, B. Clancy, L. Luo, J. Kinast, A. Turlapov, and J. E. Thomas, Phys. Rev. Lett. **98**, 170401 (2007).
[15] D. E. Miller, J. K. Chin, C. A. Stan, Y. Liu, W. Setiawan, C. Sanner, and W. Ketterle, Phys. Rev. Lett. **99**, 070402 (2007).
[16] C. Menotti, P. Pedri, and S. Stringari, Phys. Rev. Lett. **89**, 250402 (2002).
[17] S. Stringari, Europhys. Lett. **65**, 749 (2004).
[18] H. Heiselberg, Phys. Rev. Lett. **93**, 040402 (2004); H. Hu, A. Minguzzi, X.-J. Liu, and M. P. Tosi, *ibid.* **93**, 190403 (2004).
[19] R. Combescot and X. Leyronas, Phys. Rev. Lett. **93**, 138901 (2004); A. Bulgac and G. F. Bertsch, *ibid.* **94**, 070401 (2005).
[20] T. N. De Silva and E. J. Mueller, Phys. Rev. A **72**, 063614 (2005).
[21] R. Combescot, M. Y. Kagan, and S. Stringari, Phys. Rev. A **74**, 042717 (2006).
[22] M. Antezza, M. Cozzini, and S. Stringari, Phys. Rev. A **75**, 053609 (2007).
[23] Y. E. Kim and A. L. Zubarev, Phys. Rev. A **70**, 033612 (2004); **72**, 011603(R) (2005).
[24] N. Manini and L. Salasnich, Phys. Rev. A **71**, 033625 (2005).
[25] T. K. Ghosh and K. Machida, Phys. Rev. A **73**, 013613 (2006); **74**, 057602 (2006); P. Capuzzi, P. Vignolo, F. Federici, and M. P. Tosi, *ibid.* **74**, 057601 (2006).
[26] J. Yin, Y.-L. Ma, and G. Huang, Phys. Rev. A **74**, 013609 (2006).
[27] Y.-L. Ma and G. Huang, Phys. Rev. A **75**, 063629 (2007).
[28] W. Wen and G. Huang, Phys. Lett. A **362**, 331 (2007).
[29] Y. Zhou and G. Huang, Phys. Rev. A **75**, 023611 (2007).
[30] A. Altmeyer, Ph.D. thesis, Universität Innsbruck, 2007.
[31] F. Dalfovo, C. Minniti, and L. P. Pitaevskii, Phys. Rev. A **56**, 4855 (1997).
[32] G. E. Astrakharchik, J. Boronat, J. Casulleras, and S. Giorgini, Phys. Rev. Lett. **93**, 200404 (2004).
[33] J. Carlson, S.-Y. Chang, V. R. Pandharipande, and K. E. Schmidt, Phys. Rev. Lett. **91**, 050401 (2003).
[34] Note that the case $\gamma=2/3$ corresponds to both the BCS limit ($\eta=-\infty$) and the unitarity point ($\eta=0$).
[35] S. Stringari, Phys. Rev. Lett. **77**, 2360 (1996).
[36] D. S. Jin, J. R. Ensher, M. R. Matthews, C. E. Wieman, and E. A. Cornell, Phys. Rev. Lett. **77**, 420 (1996); D. S. Jin, M. R. Matthews, J. R. Ensher, C. E. Wieman, and E. A. Cornell, *ibid.* **78**, 764 (1997).
[37] M. O. Mewes, M. R. Andrews, N. J. van Druten, D. M. Kurn, D. S. Durfee, C. G. Townsend, and W. Ketterle, Phys. Rev. Lett. **77**, 988 (1996).
[38] F. Chevy, V. Bretin, P. Rosenbusch, K. W. Madison, and J. Dalibard, Phys. Rev. Lett. **88**, 250402 (2002).
[39] See A. H. Nayfeh, *Perturbation Methods* (Wiley-Interscience, New York, 2000).
[40] G. Huang, X.-Q. Li, and J. Szeftel, Phys. Rev. A **69**, 065601 (2004); Y.-L. Ma, G. Huang, and B. Hu, *ibid.* **71**, 043609 (2005).
[41] R. W. Boyd, *Nonlinear Optics* (Academic, San Diego, CA, 2003).
[42] G. Hechenblaikner, O. M. Maragó, E. Hodby, J. Arlt, S. Hopkins, and C. J. Foot, Phys. Rev. Lett. **85**, 692 (2000).